Colloid Polym Sci (2002) 280: 744–750
DOI 10.1007/s00396-002-0680-5

ORIGINAL CONTRIBUTION

Jung-Bae Jun
Chung-Hyuk Lee
Jin-Woong Kim
Kyung-Do Suh

Synthesis and characterizations of monodispersed micron-sized polyaniline composite particles for electrorheological fluid materials

Received: 22 September 2001
Accepted: 12 February 2002

J.-B. Jun · C.-H. Lee · K.-D. Suh (✉)
Division of Chemical Engineering,
College of Engineering,
Hanyang University,
Seoul 133-791, Korea
E-mail: kdsuh@hanyang.ac.kr
Tel.: +82-2-22900526
Fax: +82-2-22952102

J.-W. Kim
Cosmetics Research Institute,
Pacific Corporation R&D Center,
314-1 Bora-ri, Kiheung-eup,
Yongin-si, Kyunggi-do 449-900, Korea

Abstract Monodispersed micron-sized polyaniline (PANi) composite particles were synthesized by chemical oxidation polymerization of aniline in the presence of functional porous polymer particles considering the surface functionality and the deposition space. The PANi particles formed in the reaction medium deposited onto the porous substrate to produce PANi-coated composite particles. The formation of the composite was confirmed by Fourier transform IR spectroscopy and UV–vis spectroscopy, and their morphological structures were examined by scanning electron microscopy. From the experimental results, it was determined that PANi was successfully coated onto the functional macroporous polymer particles, maintaining the size monodispersity. The electrorheological properties of the suspensions prepared by dispersing the composite particles in silicone oil were investigated under different electric fields. It was found that the fluids showed a great increase in shear stress, exhibiting a dynamic yield stress under high electric fields; however, the shear stress at low electric fields did not show good particle polarization with fluctuating stress values. In addition, the PANi composite particles exhibited different electrorheological behavior according to the particle size.

Keywords Electrorheology · Polyaniline composite particles · Size monodispersity

Introduction

An electrorheological (ER) fluid, which behaves like a Bingham fluid under an applied electric field, is generally composed of polarizable solid particles dispersed in an insulating oil [1, 2, 3, 4]. The dispersed particles form chain structures along the applied electric field, inhibiting the fluid flow, and the fluid exhibits an enhanced shear stress and, in particular, develops a yield stress at zero-shear rate. This rheological property makes various applications possible in the area of mechanics, such as damping systems, clutches, valves, positioning, and so on. Despite the great potential of ER technology, no versatile ER devices have reached the marketplace. When formulating the ER fluid for a specific application, some requirements must be satisfied, which are high yield stress under electric field and low zero-field viscosity, wide operating temperature, rapid response, and dispersion stability.

Anhydrous ER suspensions acquired a dramatic improvement over earlier wet-based ER fluids that required water or polar additives to demonstrate ER activity and lost the activity at higher working temperatures [5, 6]. As anhydrous ER fluids, suspensions of semiconducting polymers, such as polyaniline (PANi) [7, 8, 9, 10, 11] and pyrolyzed hydrocarbons [12], are the leading polarizable materials. Among those anhydrous ER fluids, PANi has attracted wide interest from many researchers because of its synthetic versatility, thermal stability, and the ability to tailor electrical properties.

Generally, dedoped or deprotonated PANi, which is called the emeraldine base form, has been widely used in ER fluids since it can be polarized more easily owing to its semiconjugated π system [8, 9]. PANi-based suspensions also achieve appreciable yield stress over a wide temperature range. However, all the PANi particles used have poor processibility and had irregular shape and size. In order to enhance the processibility of PANi, many efforts have been made regarding the preparation of colloidal PANi [13, 14], the incorporation of side groups into the main chain [15], and the use of different kinds of dopants [16].

In our previous study [17], we easily solved both the processing problem and the morphological unevenness of PANi by synthesizing monodispersed micron-sized PANi composite particles. The composite particles were obtained by polymerizing aniline monomer in the presence of preformed polymer latex particles, resulting in in situ deposition of growing PANi onto the substrate particles. The key factors for stable and clean coating of PANi are substrate functionality and the volume of deposition site that is produced by the porous structure. Hence, monosized functional porous polymer particles as a substrate were used to satisfy these factors, and finally monodispersed PANi composite microspheres could be obtained. These semiconducting composite particles have many advantages as a controlled polarization body in the field of ER fluid systems with the controllability of their composite constituent, composition ratio, conductivity, and size. In this study, we synthesized and characterized monodispersed PANi composite particles and investigated the ER properties of the corresponding suspensions. The shear-stress behavior of the ER fluid was studied as a function of the electric field strength and the particle size.

Experimental

Materials

Styrene (St, Aldrich Chemical Co.), divinylbenzene (DVB, 55% assay, Aldrich), and glycidyl methacrylate (GMA, Aldrich) were purified through a removing column before use. Aniline (Aldrich), ethanol (J.T. Baker), 2-methoxyethanol (Kanto Chemical Co.), and 1-chlorododecan (CD, Tokyo Chemical Industry Co.) were all reagent grade. Poly(vinyl pyrrolidone) ($M_w = 4.0\times10^4$ gmol^{-1}, Sigma Chemical Co.) and poly(vinyl alcohol) (PVA, $M_w = 8.8\times10^4$–9.2×10^4 gmol^{-1}, 87–89% hydrolyzed, Kuraray Co.) were used as polymeric stabilizers, and di-2-ethylhexyl ester of sodium sulfosuccinic acid (Aerosol-OT, American Cyanamid) was used as a costabilizer. 2,2-Azobis(isobutyronitrile) (AIBN) and benzoyl peroxide (BPO) were purchased from Junsei Chemical Co. and were recrystallized from methanol, and ammonium persulfate (APS, Tokyo Chemical Industry Co.) was used as received.

Preparation of uniform porous polymer particles

Highly monodispersed polystyrene (PS) seed particles were prepared by dispersion polymerization based on our previous polymerization condition [18, 19]. The type of dispersion medium was changed to obtain monodispersed seed particles with different diameters. Two different dispersion polymerization recipes were applied and they are summarized in Table 1. These PS seed particles with different sizes were used to control the final size of the porous polymer particles.

A two-step seeded polymerization procedure was used for the synthesis of uniform micron-sized poly(St-*co*-GMA-*co*-DVB) macroporous particles [20]. First, PS seed particles redispersed in 0.25 wt% sodium lauryl sulfate (SLS) aqueous solution (40 g) by sonication were swollen with CD (0.5 g) emulsified by ultrasonic homogenization in 0.25 wt% SLS aqueous solution (10 g) for 12 h. All the swelling processes were carried out at 30 °C with a mechanical stirring speed of 200 rpm. After the complete disappearance of CD emulsion droplets, the mixture of St (1.0 g), GMA (2.0 g), DVB (3.0 g), toluene (4.0 g), and BPO (1.0 wt% against total monomers) was emulsified by the previously described emulsification method and poured into the reactor. The monomer-swollen particles were then stabilized with 5.0 wt% PVA aqueous solution and the PVA concentration was fixed at 1.0 wt% of the total weight (250 g). Polymerization in the aqueous phase was inhibited by adding copper(II) chloride (0.2 g). After deaeration with nitrogen gas, the polymerization was carried out at 80 °C for 10 h. The particles produced were washed repeatedly with water and ethanol. Soxhlet extraction was performed using methylene chloride for 36 h to eliminate linear seed polymer and other impurities.

Synthesis of PANi composite particles

Epoxy-functionalized porous particles (2 g) were dispersed in 1 M HCl aqueous solution (180 g) with magnetic stirring in a screw-capped bottle. Then, aniline monomer (0.5 g) was added to the dispersion and a prechilled solution (20 g) of APS (1.47 g) in 1 M HCl was added at once; the polymerization reaction was continued at about 5 °C for 12 h. The molar ratio of APS to aniline was fixed at 1. The synthesized composite particles were separated through centrifugation and washed several times with water to remove the initiator and unreacted monomer. Then, the PANi composites were immersed in 3 wt% ammonia water with continuous stirring for 3 h to obtain the emeraldine base form of PANi. The product was finally dried in a vacuum oven at 80 °C for 1 day. All the composite particles had a PANi loading of 20 wt%.

Characterization of the particles

Identification of the composite particles was performed by Fourier transform (FT) IR (Mahgna IR-550, Nicolet) spectroscopy and UV–vis spectroscopy (UV S-2100, Scinco Co.). The surface morphology of the composite was observed with a scanning electron

Table 1. Standard recipe for dispersion polymerization. 70 °C; 24 h; 12.5 wt% monomer concentration based on total weight. 2,2-Azobis(isobutyronitrile) (*AIBN*) (1.0 wt% based on monomer weight) was added. Urethane acrylate (2.0 wt% based on total monomer weight) was used as a cross-linking agent

Seed latex	SL1 (g)	SL2 (g)
Styrene	12.25	12.25
AIBN	0.125	0.125
Urethane acrylate	0.25	0.25
PVP K-30	1.79	1.79
Aerosol-OT	0.4	0.4
Ethanol	59.70	42.64
2-Methoxyethanol	25.58	42.64

microscope (SEM, JSM-6330F, JEOL). The diameter of the particles was determined by image analysis from SEM photographs. Thermogravimetric analysis (TGA) was carried out in the temperature range of 30–700 °C at a heating rate of 20 °Cmin^{-1} under a nitrogen atmosphere using a SDT2960 (TA Instruments). The specific surface area, the pore volume, and the pore size of the porous particles were calculated from the Brunaner–Emmett–Teller isotherm of sorption/desorption of nitrogen. The molecular weight of the coated PANi in the dedoped state was determined using Styragel HR 1–4 columns from Waters Associates at 25 °C.

Preparation and rheological measurements of ER fluids

ER suspensions with 20% weight fraction were prepared by dispersing the PANi composite particles in silicone oil (KF-96, 100 cS, Shinetsu) using mechanical stirring. The rheological behavior of the ER suspensions was determined under direct current electric fields using a rotational Physica rheometer (MC120) with Couette-type geometry along with a high-voltage power supply (HVG 5000) at room temperature. The ER fluids were placed in the gap between the stationary outer cup and the inner rotating bob. An electric field was applied for 5 min in order to obtain an equilibrium structure before applying the shear. The shear rate was varied from 10^{-1} to 10^{3} s^{-1} and the flow curves were obtained with the rheometer operating in the controlled-shear-rate (CSR) mode. Electric current going through the ER fluid was measured using a Keithley 196 system.

Results and discussion

Monodispersed micron-sized PANi composite particles

Monodispersed and stable seed particles were obtained by dispersion polymerization. SEM photographs of the PS seed latexes with different two sizes used in the preparation of the porous polymer particles are shown in Fig. 1. All the seed particles were very clear and highly monodisperse with a particle size distribution of 1.01. 2-Methoxyethanol was used to alter the medium solvency and, consequently, to control the size of the seed particles. Ober and Hair [21] stated that the mechanism for particle nucleation in dispersion polymerization depends heavily on the molecular weight of polymer produced by the polymerization before the initial precipitation, which is dependent on the solvency of the reaction medium. If fewer chains precipitate to form nuclei at higher medium solvency, larger particles will eventually result; therefore, the particle size can be adjusted by controlling the medium solvency. In reality, the number-average particle sizes obtained were 2.87 and 5.01 μm for SL1 and SL2 seed latexes, respectively.

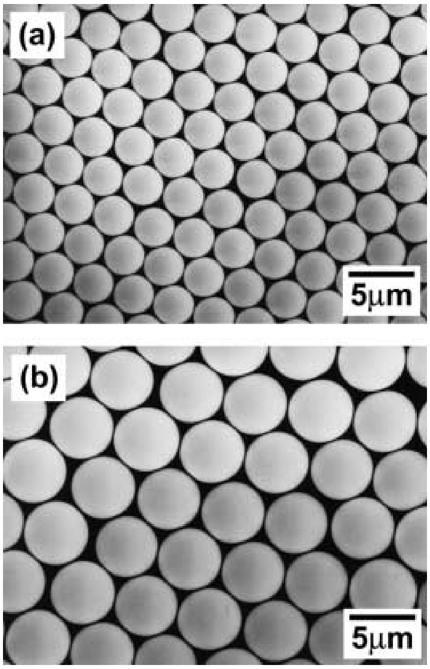

Fig. 1. Scanning electron microscope (*SEM*) photographs of polystyrene (*PS*) seed particles: **a** SL1 and **b** SL2

With these seed particles, monodispersed porous polymer particles with three different sizes were produced by changing either the type of seed latex or the monomer-swelling ratio in the two-step seeded polymerization. The properties of the porous particles produced are presented in Table 2. All the porous particles had size monodispersity and structural uniformity. In our previous work [17], a surface epoxy group and a porous structure were introduced to the substrate polymer particles in order to obtain high coating efficiency and to solve the problem of free particles forming

Table 2. Properties of porous poly(styrene-*co*-glycidyl methacrylate-*co*-divinylbenzene) particles produced with different seed latexes and swelling ratios

Sample	Seed latex	Swelling ratio[a]	Particle size		Porous properties		
			D_n (μm)[b]	D_w/D_n	A_s (m^{2}g^{-1})[c]	V_p (mlg^{-1})[d]	D_p (nm)[e]
PSG1	SL1	20	7.01	1.01	20.01	0.13	62.7
PSG2	SL2	20	12.72	1.01	16.27	0.13	58.9
PSG3	SL2	50	18.10	1.01	13.53	0.11	53.4

[a] Monomer swelling ratio against the seed latex by weight
[b] Particle size measured from scanning electron microscope photographs
[c] Specific surface area
[d] Pore volume
[e] Average pore size

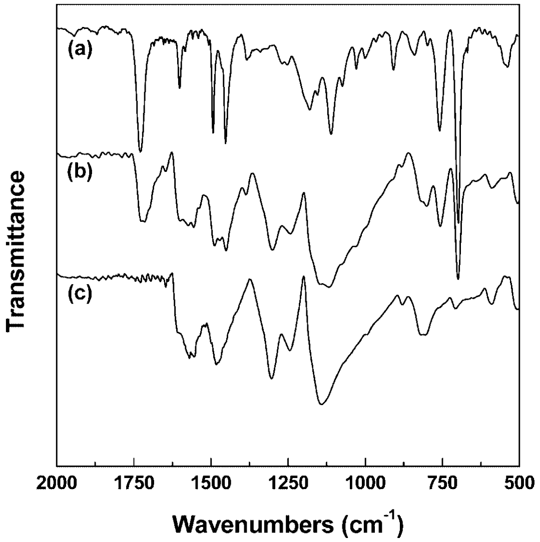

Fig. 2. Fourier transform IR spectra of porous poly(styrene-*co*-glycidyl methacrylate-*co*-divinylbenzene) particles (*a*) and the corresponding monodispersed micron-sized polyaniline (*PANi*) composite particles (*b*), and pure PANi particles (*c*)

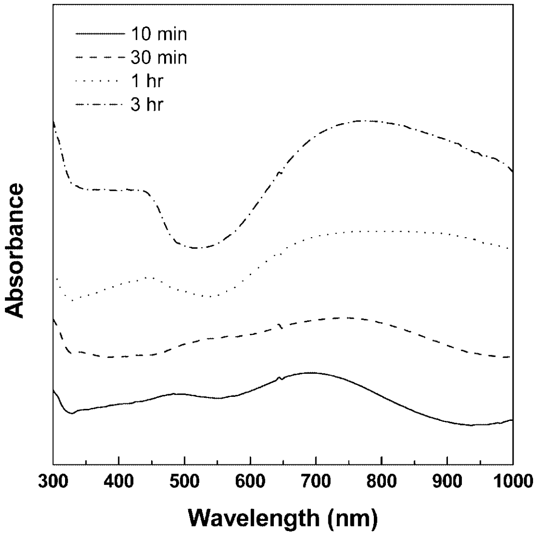

Fig. 3. UV–vis absorption spectra of samples taken at various times during the polymerization of aniline in 1 M HCl aqueous solution at about 5 °C

separately in the reaction medium. One interesting point was that uniformly coated particles could be obtained by using epoxy-functionalized porous particles with enhanced surface area and larger pores. All the particles could be characterized in the macroporous range from the results of the pore size, D_p, the pore volume, V_p, and the specific surface area, A_s. Here, the synthetic route of our previous study was followed and monodispersed PANi-coated polymer particles were successfully obtained.

The formation of PANi composite particles was confirmed by FT-IR spectra as shown in Fig. 2. After polymerizing aniline in the presence of porous polymer particles, four strong absorption bands attributed to PANi were observed at 1,555, 1,487, 1,300, and 1,140 cm^{-1}. These peaks are attributed to characteristic vibrational modes of the quinoid ring and stretching vibrations of the benzoid unit, the C–N bond, and the quinoid ring, respectively. The oxidation state of PANi during the aniline polymerization in the presence of porous particles was investigated by UV–vis spectroscopy. Typical UV–vis spectra of aniline polymerization in acidic aqueous solution with time are shown in Fig. 3. After about 30 min polymerization, the solution apparently turned blue and a slight absorption peak at 540 nm appeared, indicating the formation of protonated pernigraniline. The blue color intensified gradually with further polymerization. After 1 h polymerization, the solution turned dark green, which is associated with significant structural changes from protonated pernigraniline to the emeraldine salt form of PANi with fast depletion of oxidant $S_2O_8^{2-}$. In addition, two characteristic absorption peaks of the emeraldine salt form were observed near 450 nm and at above the 600-nm region. The absorption around 60–1,000 nm is assigned to the presence of a polaron resulting from the doping process [22, 23]. This

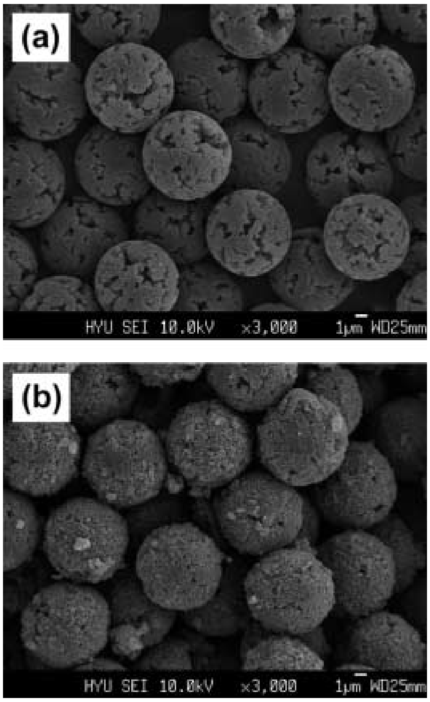

Fig. 4. SEM photographs of **a** porous polymer particles (PSG1) and **b** the corresponding PANi composite particles

Table 3. Characteristics of the monodispersed micron-sized polyaniline (*PANi*) composite particles (*PCP*)

Sample	PANi layer		Particle size		Porous properties		
	Thickness (μm)	M_w	D_n (μm)	D_w/D_n	A_s (m^2g^{-1})	V_p (mlg^{-1})	D_p (nm)
PCP1	0.44	31,700	7.45	1.01	19.91	0.09	18.1
PCP2	0.42	32,100	13.14	1.02	17.69	0.09	20.2
PCP3	0.50	31,800	18.60	1.02	17.48	0.08	14.1

indicates that the coated PANi layer exists in the doped state of the emeraldine form.

SEM photographs of porous polymer particles (PSG1 in Table 2) and the corresponding PANi composite particles are shown in Fig. 4. The overall coating of the porous particle with PANi is shown in Fig. 4b. The characteristics of the PANi composites are summarized in Table 3. In all cases, gel permeation chromatography of the coated PANi displayed a weight-average molecular weight of nearly 32,000. The particle size distribution of the porous particles was very narrow and monodispersity was also maintained in the composite particles. This reveals that the PANi composite particles are colloidally very stable at a PANi loading of 20 wt%. In the cases studied earlier [24, 25], conducting polymer-coated polymer latexes exhibited coagulated particle morphologies at a loading of 20 wt% or above. This problem was successfully resolved by using porous substrate particles providing larger deposition space.

TGA thermograms for pure PANi, porous polymer particles, and the PANi composite particles are shown in Fig. 5. Colloidal pure PANi showed monotonic mass loss over a wide temperature range, exhibiting three characteristic mass-loss regions. The initial mass loss between 50 and 140 °C was usually associated with moisture release [26] and further mass loss between 170 and 280 °C was mainly due to the evolution of the dopant HCl [27]. Again a sharp mass loss above 350 °C presumably corresponds to large-scale thermal degradation of PANi main chains [26]; nearly 36% residue was left for PANi at 700 °C. This thermal behavior was also observed in the PANi composite particles. The thermogram of the PANi composite particles exhibited three slight mass-loss regions related to pure PANi and one sharp mass-loss region related to porous substrate particles. The composite left a residue of about 11% at 700 °C. PANi was successfully introduced to the substrate particles quantitatively according to the amount of aniline. The TGA data indicate that the PANi layer of the composite was not far from the colloidal pure PANi which has been used as ER materials.

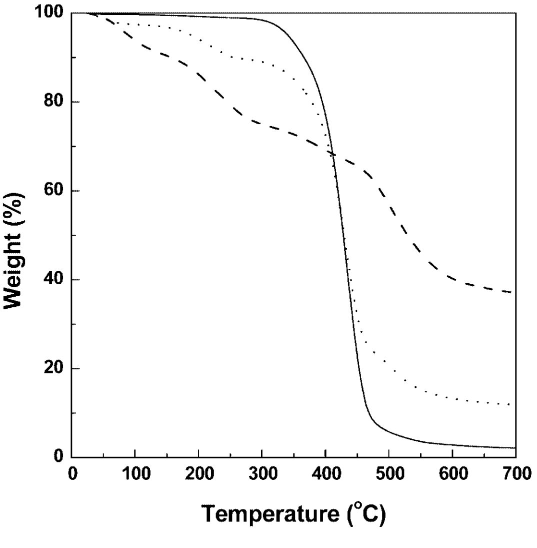

Fig. 5. Thermogravimetric analysis thermograms of porous polymer particles (*solid line*), HCl-doped pure PANi (*dashed line*), and the PANi composite particles (*dotted line*)

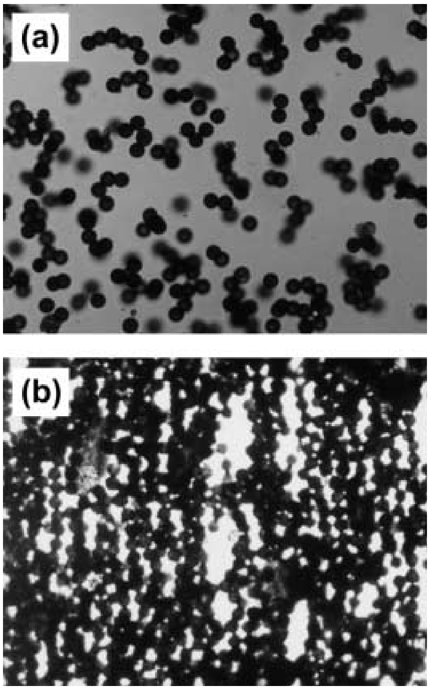

Fig. 6. Optical micrographs of 5 wt% suspension of PANi composite particles **a** before and **b** after the application of an electric field (1 $kVmm^{-1}$)

ER properties of the PANi composite suspensions

Micrographs of the suspensions before and after application of an electric field confirm the transition of randomly dispersed particles to the organized chain structure of particles (Fig. 6). When an electric field was applied, the particles were polarized and immediately formed many chains (clusters) bridging the two electrodes. This chain structure causes an increase in the shear stress.

The flow curves of the shear stress, τ, versus the shear rate, $\dot{\gamma}$, from the CSR experiment for the suspension of PANi composite particles (PCP2) at various electric field strengths are illustrated in Fig. 7. At zero electric field, the flow curve was slightly pseudoplastic, suggesting the formation of a structure of aggregated particles, which is broken by the shear forces in the flow field [28]. When an electric field was applied to the suspensions, the shear stress abruptly increased over the entire shear rate range, exhibiting a yield stress as in a Bingham fluid. As the electric field strength increased, the shear stress at very low shear rate ($\dot{\gamma} = 0.1$) increased consecutively, and the increased yield stress was maintained at high shear rate. However, the shear stress increased above a shear rate of 30 s^{-1}. The stress behavior of the fluid is thought to be largely dominated by the hydrodynamic force generated by shear beyond this shear-rate region. At lower electric field strengths of 1 and 2 $kVmm^{-1}$, the shear stress exhibited fluctuating values. This is probably due to the repetition of structural chain formation/deformation of suspended particles, which indicates that the interparticle interaction force is not so strong at low electric fields as to resist the shear force even in the low-shear-rate range.

The conductivity of the dedoped PANi composite particles was measured using a four-probe conductometer and all the values were approximately 2.0×10^{-10} Scm^{-1}. The current density of the PANi composite suspension as a function of electric field strength is shown in Fig. 8. The suspension showed relatively low current densities over the applied electric fields and the current density moderately increased with the field strength. It is noticeable that current density of the suspension slightly jumped up at an electric field of 3 $kVmm^{-1}$, at which the suspension started to display enhanced shear stress as shown in Fig. 7.

The present PANi composite particles have a core–shell-type structure and the particle size can be controlled as required by altering the substrate particle size. The average diameters and particle size distributions of the composites are listed in Table 3. The suspension of monodispersed PANi-coated particles was expected to become an excellent model system for studying the effect of the particle size on the ER response, and the relationship between the particle size and the stress behavior under an electric field is shown in Fig. 9. The dynamic yield stress, τ_y, can generally be obtained by extrapolating the shear rate to zero; here, the plateau stress at the lowest shear rate was regarded as a yield stress. This value is referred to as the parameter incorporating the interparticle interactions, especially in the fluid under direct current fields. At low field strengths (1 and 2 $kVmm^{-1}$), the fluids did not show any plateau stress; therefore, the stress behavior at high electric field strengths (3 and 4 $kVmm^{-1}$) was considered. As the particle size increased, the dynamic yield stress also increased in this size range. Though the

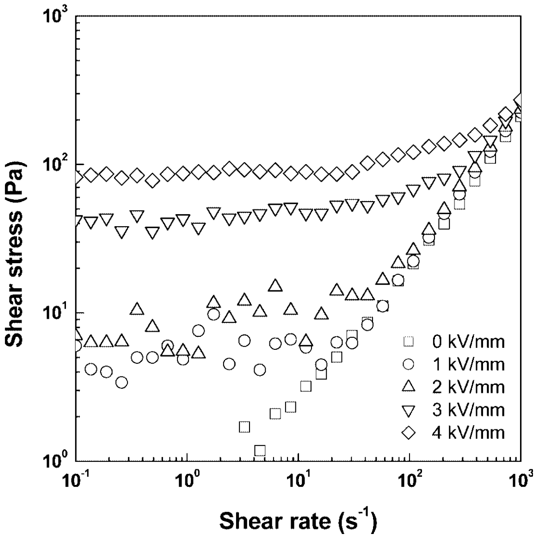

Fig. 7. Flow curves of shear stress versus shear rate for 20 wt% suspension of PANi composite particles (PCP2) at different electric fields

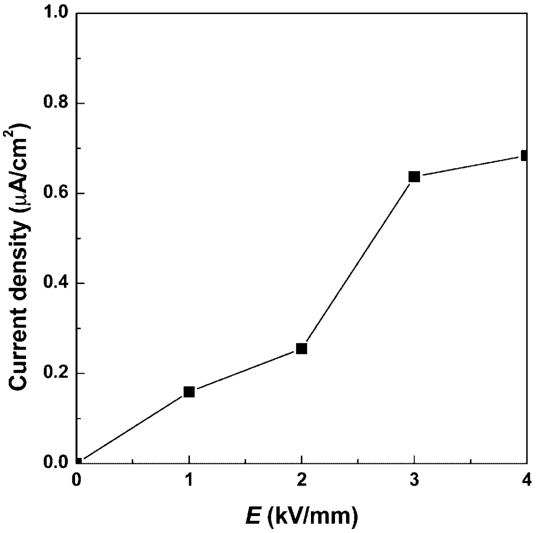

Fig. 8. Current density of the PANi composite suspension as a function of electric field strength, *E*

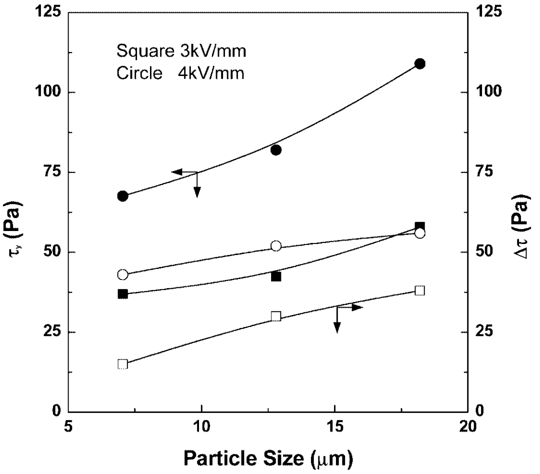

Fig. 9. Effect of particle size on the dynamic yield stress, τ_y, and the increment of shear stress, $\Delta\tau$, at $\dot{\gamma} = 728\,s^{-1}$ for 20 wt% suspensions of the monodispersed PANi composite particles

stress behavior for particles smaller than 7 μm and larger than 20 μm was not observed, there will be an optimum size revealing the maximum yield stress. In addition, the increment of the shear stress, $\Delta\tau$, also increased with the particle size in the very high shear rate region.

Conclusions

From the results of IR and UV–vis spectroscopy, thermal analysis, and image analysis, monodispersed micron-sized PANi-coated particles were successfully prepared by using functional macroporous polymer particles as a substrate. The PANi layer of the composite was found to exist in the emeraldine state, which was reported to give good polarizability. The ER fluid of PANi composite particles showed typical ER characteristics; the shear stress increased with the applied electric field. Furthermore, it was shown that the shear stress increased with the particle size in the range from 7.45 to 18.60 μm. This PANi composite-based fluid is expected to become a novel material in the systematic analysis of the ER effect because of its size monodispersity and ability to control the particle characteristics, such as the PANi content, the particle conductivity, the particle size, and the size distribution.

Acknowledgement This work was supported by the Brain Korea 21 Project.

References

1. Winslow WM (1949) J Appl Phys 20:1137
2. Block H, Kelly JP (1988) J Phys D Appl Phys 21:1661
3. Halsey TC (1991) Science 258:761
4. Gast AP, Zukoski CF (1989) Adv Colloid Interface Sci 30:153
5. Uejima H (1972) Jpn J Appl Phys 11:319
6. Otsubo Y (1991) J Colloid Interface Sci 146:395
7. Gow CJ, Zukoski CF (1990) J Colloid Interface Sci 136:175
8. Block H, Kelly JP, Qin A, Watson T (1990) Langmuir 6:6
9. Akhavan J, Slack K, Wise V (1999) Int J Mod Phys B 13:1931
10. Kuramoto N, Yamazaki M, Nagai K, Koyama K (1994) Thin Solid Films 239:169
11. Kuramoto N, Yamazaki M, Nagai K, Koyama K (1995) Rheol Acta 34:298
12. Ishino Y, Maruyama T, Ohsaki T (1995) In: Havelka KO, Filisko FE (ed) Progress in electrorheology. Plenum, New York, pp 137–145
13. Cooper EC, Vincent B (1989) J Phys D Appl Phys 22:1580
14. Armes SP, Aldissi M (1989) J Chem Soc Chem Commun 38
15. DeArmitt C, Armes SP, Winter J, Uribe FA, Gottesfels S, Mombourquette C (1993) Polymer 34:158
16. Cao Y, Smith P, Heeger AJ (1992) Synth Met 48:91
17. Jun JB, Kim JW, Lee JW, Suh KD (2001) Macromol Rapid Commun 22:937
18. Kim JW, Suh KD (1998) Colloid Polym Sci 276:870
19. Kim JW, Suh KD (2000) Polymer 41:6181
20. Ryu JH, Kim JW, Suh KD (2001) Colloid Polym Sci 279:146
21. Ober CK, Hair ML (1987) J Polym Sci A Polym Chem 25:1395
22. Sun Y, MacDiarmid AG, Epstein AJ (1990) J Chem Soc Chem Commun 529
23. Stejskal J, Kratochvil P, Radhakrishnan N (1993) Synth Met 61:225
24. Lascelles SF, Atmes SP (1997) J Mater Chem 7:1339
25. Barthet C, Armes SP, Lascelles SF, Luk SY, Stanley HME (1998) Langmuir 14:2032
26. Chan HSO, Ng SC, Sim WS, Tan KL, Tan BTG (1992) Macromolecules 25:6029
27. Chan HSO, Ng SC, Sim WS, Seow SH, Tan KL, Tan BTG (1993) Macromolecules 26:144
28. Pavlínek V, Quadrat O, Porsch B, Sáha P (1999) Colloid Surf A 155:241